Published in final edited form as:
Crit Care Med. 2009 June ; 37(6): 1978–1987. doi:10.1097/CCM.0b013e31819feb4d.

Lung injury after hemorrhage is age-dependent: role of peroxisome proliferator activated receptor γ

Basilia Zingarelli, MD, PhD[1], **Paul W. Hake**[1], **Michael O'Connor**[1], **Timothy J. Burroughs**[1], **Hector R. Wong, MD**[1], **Joseph S. Solomkin, MD**[2], and **Alex B. Lentsch, PhD**[2]

[1]Division of Critical Care Medicine, Cincinnati Children's Hospital Medical Center, Department of Pediatrics, College of Medicine, University of Cincinnati, Cincinnati, Ohio.

[2]Laboratory of Trauma, Sepsis & Inflammation Research, Department of Surgery, College of Medicine, University of Cincinnati, Cincinnati, Ohio.

Abstract

Objective—The incidence of multiple organ failure in pediatric trauma victims is lower than in the adult population. However, the molecular mechanisms are not yet defined. We investigated whether the pathophysiologic characteristics of hemorrhage-induced lung injury may be age-dependent and may be regulated by the peroxisome proliferator activator receptor γ (PPARγ).

Design—Prospective, laboratory investigation that used an established rodent model of hemorrhagic shock.

Setting—University hospital laboratory.

Subjects—Young (n=67; 3–5 months old) and mature (n=66; 11–13 months old) male rats.

Interventions—Hemorrhagic shock was induced in young and mature rats by withdrawing blood to a mean arterial blood pressure of 50 mmHg. After 3 hrs, rats were rapidly resuscitated by infusing the shed blood and sacrificed 3 hrs thereafter.

Measurements and Main Results—In young rats, lung injury was characterized by accumulation of red cells and neutrophils at the end of the resuscitation period; at Western blot analysis, lung expression of intercellular adhesion molecule-1 (ICAM-1) was increased. In contrast, the severity of lung injury was more pronounced in mature rats. Lung myeloperoxidase activity and expression of constitutive and inducible ICAM-1 was significantly higher in mature rats when compared to young rats. Mature rats also had higher plasma levels of cytokines and chemokines when compared to young rats. This heightened inflammation was associated with higher degree of activation of nuclear factor-κB and down-regulation of PPARγ and heat shock factor-1 in the lung of mature rats when compared to young rats. Treatment with the PPARγ ligand, the cyclopentenone prostaglandin 15-deoxy-$\Delta^{12,14}$-prostaglandin J_2, ameliorated lung injury in young, but not in mature animals.

Conclusions—Lung injury after severe hemorrhage is age-dependent and may be secondary to a diverse regulation of PPARγ.

Keywords

acute lung injury; aging; hemorrhage; heat shock factor-1; nuclear factor-κB; peroxisome proliferator-activated receptor-γ

Address correspondence to: Basilia Zingarelli, M.D., Ph.D., Cincinnati Children's Hospital Medical Center, Division of Critical Care Medicine, 3333 Burnet Avenue, Cincinnati, Ohio 45229, Tel.: 513 636 8704; Fax: 513 636 4892, E-mail: basilia.zingarelli@cchmc.org.

INTRODUCTION

Shock consequent to trauma and severe hemorrhage is a systemic inflammatory response characterized by hemodynamic and metabolic derangements that may result in multiple organ dysfunction syndrome (MODS) and death. This clinical scenario is characterized by an overwhelming production of inflammatory mediators and by migration and sequestration of activated neutrophils into tissues and organs. A common clinical observation is that pediatric patients have lower incidence of MODS than adult trauma victims (1,2). In addition to the incidence, the character of MODS in pediatric victims is different from adults. For example, traumatized pediatric patients appear to have lower incidence of acute respiratory distress syndrome and to recover faster than adult victims. This is different from adults, who usually require assisted ventilation, complex intensive care and a long-term recovery period (weeks or months) (1,3). Despite these observations, no scientific data are available to support whether molecular mechanisms of the systemic inflammatory response and development of lung injury are age-dependent.

Production of endogenous pro-inflammatory mediators and expression of adhesion molecules and chemokines is regulated at the transcriptional level by a rapid activation of the transcription nuclear factor-κB (NF-κB). Enhanced DNA binding of NF-κB has been demonstrated in the lung and appears to contribute to the development of acute lung injury after hemorrhage in experimental animals (4–6). On the contrary, in conditions of oxidative stress the heat shock transcriptor factor-1 (HSF-1) attempts to provide cytoprotection in several organs against inflammatory insults through increased expression of heat shock proteins (HSPs) (7).

Peroxisome proliferator activated receptor-γ (PPARγ) is a nuclear receptor that functions directly as a transcription factor to control gene regulation for adipocyte proliferation, glucose homeostasis and atherosclerosis (8). Experimental studies also support a modulatory role for PPARγ in inflammation in several tissues and organs, including the lung. In this regard, PPARγ ligands, such as the synthetic thiazolidinediones and the natural cyclopentenone prostaglandin 15-deoxy-$\Delta^{12,14}$-prostaglandin J_2 (15d-PGJ_2), have been shown to ameliorate lung injury during sepsis or endotoxin challenge in young mice and rats (11–14). This protective effect appeared to be related to inhibition of NF-κB (8,11–12) and activation of the heat shock response (12).

Based on these previous findings, aim of our study was to determine whether the severity of the lung inflammatory response during hemorrhagic shock is age-dependent and is modulated at the nuclear level by a diverse regulation of the PPARγ pathway.

MATERIALS AND METHODS

Hemodynamic Parameters Measurement

The investigation conformed with the *Guide for the Care and Use of Laboratory Animals* published by US National Institutes of Health (NIH Publication No. 85-23 revised 1996) and commenced with the approval of the Institutional Animal Care and Use Committee. Male Wistar rats (Charles River laboratories, Wilmington MA) weighing 225–275 g (3–5 months old, n=67) were included in the young group; rats weighing 500–700 g (11–13 months old, n=66) were included in the mature group. The animals were anesthetized with thiopentone sodium (70 mg/kg) intraperitoneally (i.p.). The trachea was cannulated to facilitate respiration and temperature was maintained at 37° C using a homeothermic blanket. The right carotid artery was cannulated (PE-50 tubing) and connected to a pressure transducer for the measurement of mean arterial blood pressure (MABP) and heart rate (HR). The right femoral artery was cannulated for withdrawal of blood. The cardiac output (mL/min) was also measured

by thermodilution technique (15). Briefly, a thermistor was passed into the carotid artery and advanced to the aortic arch. A thermal indicator (0.1 mL of normal saline at room temperature) was then injected into the right atrium via an 8-cm length of PE-50 tubing placed in the jugular vein. The pressure transducer and the cardiac output pod were connected to a Maclab A/D converter (AD instruments, Milford, MA, USA). The cardiac index (CI, mL/min/100 g), total peripheral resistance index (TPRI, mmHg/mL/min 100 g) and stroke volume index (SVI, ml/100 g) were then calculated from the computed integral values of thermodilution curves using standard arithmetic formulae.

Hemorrhagic Shock Model

Upon completion of the surgical procedure, cardiovascular parameters were allowed to stabilize for 15 min and animals received heparin (100 IU/kg) to facilitate hemorrhage. Hemorrhagic shock was performed as previously described using an experimental protocol of pressure-controlled hemorrhage (16) by withdrawing blood (approximately 0.5 ml/min) from the femoral artery into a reservoir until MABP stabilized at 50 mmHg (Fig. 1). Shed blood volume was 8.5±1.7 ml in young rats, and 14.3±1.8 ml in the mature group and corresponded approximately to 45% and 33% of total blood volume in young and mature rats, respectively. After this initial bleeding, additional small volumes of blood were withdrawn or re-transfused as necessary to maintain MABP at 50 mmHg. At 3 hrs after hemorrhage, rapid resuscitation was performed by transfusing the shed blood over a 5 min period. If small volumes of blood were needed to be re-transfused during the hypoperfusion period to maintain MABP at 50 mmHg, rapid resuscitation was performed by transfusing the remaining shed blood supplemented with Ringer lactate solution to a final volume of fluids equal to the initial total shed blood. Animals were divided in 4 groups: 1) in the *Vehicle-Hemorrhagic Shock* group, rats (young n=30; old n=35) received vehicle (100% dimethyl sulfoxide) instead of the PPARγ ligand; 2) in the *15d-PGJ$_2$ (0.5 mg)-Hemorrhagic Shock* group, rats (young n=27; old n=21) received the PPARγ ligand at 0.5 mg/kg; 3) in the *15d-PGJ$_2$ (1 mg/kg)-Hemorrhagic Shock* group, rats (young n=5; old n=5) received the PPARγ ligand at 1 mg/kg; 4) in the *Sham* group, rats (young n=5; old n=5) served as control at time 0 and underwent similar surgical preparation but were not bled. The PPARγ ligand or vehicle was administered i.p. as a bolus at the beginning of resuscitation and every hour thereafter. Time-course experiments were performed in the *Vehicle-Hemorrhagic Shock* and in the *15d-PGJ$_2$ (0.5 mg)-Hemorrhagic Shock* groups. Animals (n=3–16 for each time point) were sacrificed at 1, 2, 3 hrs after the hemorrhage during the hypoperfusion period and at 15 min, 30 min, 1, 2 and 3 hrs after the transfusion (Fig. 1). Plasma samples and lungs were collected for the histological and biochemical studies described below.

Myeloperoxidase Activity

Myeloperoxidase activity was determined as an index of neutrophil accumulation in lungs. It was defined as the quantity of enzyme degrading 1 μmol of hydrogen peroxide/min at 37°C and expressed in units per 100 mg tissue (11).

Plasma Levels of Cytokines and Chemokines

Plasma levels of TNFα were evaluated by commercially available solid-phase sandwich ELISA kits (R&D Systems, Minneapolis, MN), using the protocol recommended by the manufacturer. Plasma levels of IL-1β, IL-6, IL-10, keratinocyte-derived (KC) chemokine, and monocyte chemoattractant protein-1 (MCP-1) were determined by a multiplex array system (Linco-Research, St. Charles, MO).

Histopathological Analysis

Lungs were fixed in 4% paraformaldehyde and embedded in paraffin. Sections were stained with hematoxylin and eosin and evaluated by three independent observers unaware of the experimental protocol. Specifically, lung injury was analysed by a semi-quantitavive score as previously reported (13,14) based on the following histologic features: a) alveolar congestion; b) hemorrhage; c) infiltration or aggregation of neutrophils in airspace or vessel wall; and d) thickness of alveolar wall/hyaline membrane formation. Each feature was graded from 0 to 4 (i.e., absent, mild, moderate or severe). The four variables were summed to represent the lung injury score (total score, 0–16).

Subcellular Fractionation and Nuclear Protein Extraction

Lung samples were homogenized with a Polytron homogenizer in a buffer containing 0.32 M sucrose, 10 mM tris-HCl, pH 7.4, 1 mM EGTA, 2 mM EDTA, 5 mM NaN_3, 10 mM β-mercaptoethanol, 20 μM leupeptin, 0.15 μM pepstatin A, 0.2 mM phenylmethanesulfonyl fluoride, 50 mM NaF, 1 mM sodium orthovanadate, 0.4 nM microcystin. The homogenates were centrifuged (1,000 × g, 10 min) and the supernatant (cytosol + membrane extract) was collected for evaluation of ICAM-1 as described below. The pellets were solubilized in Triton buffer (1% Triton X-100, 150 mM NaCl, 10 mM Tris-HCl, pH 7.4, 1 mM EGTA, 1 mM EDTA, 0.2 mM sodium orthovanadate, 20 μM leupeptin A, 0.2 mM phenylmethanesulfonyl fluoride). The lysates were centrifuged (15,000 × g, 30 min, 4°C), and the supernatant (nuclear extract) was collected for evaluation of content of PPARγ, and DNA binding of PPARγ, NF-κB and HSF-1.

Western Blot Analysis

Nuclear content of PPARγ and cytosol content of ICAM-1 in the lung were determined by immunoblot analyses on nitrocellulose membranes using primary antibodies against PPARγ or ICAM-1 and secondary peroxidase-conjugated antibody. Membranes were also reprobed with primary antibody against β-actin to ensure equal loading samples. Immunoreaction was visualized by chemiluminescence. Densitometric analysis of blots was performed using ImageQuant (Molecular Dynamics, Sunnyvale, CA).

Electrophoretic Mobility Shift Assay (EMSA)

EMSAs were performed as previously described (11). Oligonucleotide probes corresponding to NF-κB consensus sequence (5'-AGT TGA GGG GAC TTT CCC AGG C-3'), to HSF-1 consensus sequence (5'-GCC TCG AAT GTT CGC GAA GTT TCG-3') or PPARs consensus sequence (5'-GAA AAC TAG GTC AAA GGT CA-3') were labeled with γ-[^{32}P]ATP using T4 polynucleotide kinase and purified in Bio-Spin chromatography columns (BioRad, Hercules, CA). Ten μg of nuclear protein were preincubated with EMSA buffer (12 mM HEPES pH 7.9, 4 mM Tris-HCl pH 7.9, 25 mM KCl, 5 mM $MgCl_2$, 1 mM EDTA, 1 mM DTT, 50 ng/ml poly [d(I-C)], 12% glycerol v/v, and 0.2 mM PMSF) on ice for 10 min before addition of the radiolabeled oligonucleotide for an additional 10 min. The specificity of the binding reactions was determined by co-incubating duplicate nuclear extract samples with 100-fold molar excess of respective unlabeled oligonucleotides (competitor assays). Supershift assays, to further determine the specificity of binding, was performed by co-incubating samples with antibodies corresponding to HSF-1, PPARα, PPARβ/δ or PPARγ. Protein-nucleic acid complexes were resolved using a non-denaturing polyacrylamide gel consisting of 5% acrylamide (29:1 ratio of acrylamide:bisacrylamide) and run in 0.5X TBE (45 mM Tris-HCl, 45 mM boric acid, 1 mM EDTA) for 1 h at constant current (30 mA). Gels were transferred to Whatman 3M paper, dried under a vacuum at 80°C for 1 h, and exposed to photographic film at −70°C with an intensifying screen. Densitometric analysis was performed using ImageQuant (Molecular Dynamics, Sunnyvale, CA).

Materials

The primary antibody directed at ICAM-1 and the oligonucleotides for NF-κB and PPARs were obtained from Santa Cruz Biotechnology, Inc. (Santa Cruz, CA). The primary antibody directed at PPARγ and the compound 15d-PGJ_2 was obtained from Biomol Research Laboratories (Plymouth Meeting, PA). The primary antibody directed at β-actin was obtained from Abcam (Cambridge, MA). The oligonucleotide probe for HSF-1 corresponded to a previously published heat shock element consensus sequence (17) and was synthesized by the University of Cincinnati DNA Core Facility. All other chemicals were from Sigma/Aldrich (St. Louis, MO).

Data Analysis

Data was analyzed using SigmaStat for Windows Version 3.10 (SysStat Software, San Jose, CA). Values in the figures and text are expressed as mean ± SEM of *n* observations, where *n* represents the number of animals in each group. Specifically, hemodynamic data were analyzed using a general linear model for repeated measures allowing for missing data. For the remainder of the data analysis, a two factor ANOVA followed by Bonferroni's correction test was utilized. Statistical analysis of damage scores was performed using the Mann-Whitney U test. A value of $p < 0.05$ was considered significant.

RESULTS

Hemodynamic Parameters during Hemorrhagic Shock

As shown in Table 1, age-related changes in hemodynamic parameters were evident under basal conditions, as mature rats exhibited higher values of MABP and TPRI, and lower values of CI and SVI when compared with young rats. At the end of hemorrhage (180 min), MABP, CI and SVI declined in a similar fashion both in young and mature animals. After blood re-transfusion, CI and SVI returned toward baseline level in mature rats within the first hour. CI and SVI were partially recovered in young rats, but did not complete return to baseline. HR or TPRI did not change significantly during the hypoperfusion or resuscitation period.

Age-Dependent Differences in Cytokine and Chemokine Production

Plasma levels of cytokines and chemokines were measured at the end of hemorrhage period and at the end of the resuscitation period. Mature rats exhibited a substantial increase in plasma levels of TNFα at the end of hemorrhage, and IL-1β after resuscitation. Levels of IL-6 were similar in both groups. Production of IL-10, KC and MCP-1were significantly higher in young rats (Fig. 2).

Age-Dependent Lung Injury and Neutrophil Infiltration

At histological examination, alveolar space appeared normal in both age groups of rats under basal conditions. However, sham mature rats exhibited a modest neutrophil infiltration and thickening of the alveolar walls when compared to young rats. After hemorrhage and resuscitation in young rats, lung injury was characterized by reduction of alveolar space and accumulation of inflammatory cells. In mature rats, lung injury was more pronounced with extravasation of erythrocytes and inflammatory cells (Fig. 3A–D; Fig. 7B for injury score). In a time-course analysis, we found that myeloperoxidase activity, an index of neutrophil infiltration, increased in the lung as early as 2 hrs after hemorrhage and was further enhanced after resuscitation in the young group. Interestingly, the degree of myeloperoxidase activity was significantly more pronounced in mature rats at basal conditions and after resuscitation when compared to young rats, thus suggesting a massive neutrophil infiltration (Fig. 3E).

Age-Dependent Lung Expression of ICAM-1

Since neutrophil recruitment may be regulated by ICAM-1 (18), we evaluated the lung expression of this adhesion molecule after hemorrhage and resuscitation. Western blot analysis revealed that lung expression of both constitutive and inducible ICAM-1 was more pronounced in mature rats when compared to the expression in young animals (Fig. 4). Thus, these data suggest that an up-regulation of adhesion molecules may be responsible for the massive neutrophil infiltration observed in mature animals.

Age-Dependent Lung Activation of NF-κB and HSF-1

To investigate the molecular mechanisms underlying the pronounced susceptibility to hemorrhage of mature animals, we evaluated the activation of NF-κB, a major transcription factor involved in the signal transduction of inflammatory mediators (19), and the activation of HSF-1, which regulates the defense mechanism of the heat shock response (7). As shown in Fig. 5A, DNA binding of NF-κB in the lung of young rats increased at 3 hrs after hemorrhage and was further enhanced within 15–30 min after resuscitation and declined thereafter. In the lung of mature rats, activation of NF-κB exhibited similar kinetics, increasing after hemorrhage and the early period of resuscitation. However, the degree of activation was more pronounced in the older group of animals (Fig. 5A). On the contrary, in young rats subjected to hemorrhage, we observed that DNA binding of HSF-1 increased in the lung in a time-dependent manner after blood resuscitation and was more pronounced when compared with activation of HSF-1 of mature rats (Fig. 5B).

Age-Dependent Lung Expression of PPARγ

As the nuclear receptor PPARγ has been proposed to play a crucial role in the control of the inflammatory response, we investigated whether induction of hemorrhage was also associated with changes in PPARγ expression. By Western blot analysis, we observed that nuclear content of PPARγ in lungs decreased at 3 hrs after induction of hemorrhage, it increased within 1 h after resuscitation and declined progressively thereafter in young rats. Interestingly, the degree of downregulation of this receptor was more pronounced in mature rats when compared with the young group (Fig. 6). Based on the above observations, we next investigated whether down-regulation of the protein expression is also associated with changes in the DNA binding activity of PPARγ. As shown in Fig. 6, under basal conditions in the lung of a sham young rat (i.e. at time 0) there was a constitutive DNA binding activity of PPARγ, while no activity was detected in the sham old rat, thus confirming the scarce availability of protein as evidenced by Western blotting. However, in the lung of young rats, DNA binding of PPARγ increased after the end of hemorrhage and early resuscitation (15 min), declining thereafter and rising again at 2 hrs after resuscitation. In mature rats, DNA binding activity exhibited similar kinetics when compared with the young rats. However, the degree of activity was markedly less.

Effect of the PPARγ Ligand 15d-PGJ$_2$ on Hemodynamics and Lung Injury

On the basis of these findings, we examined the potential anti-inflammatory effects of the natural PPARγ ligand 15d-PGJ$_2$ in hemorrhagic shock. Treatment with 15d-PGJ$_2$ ameliorated MABP, without altering other hemodynamic parameters, in the young group only. Mature rats treated with the PPARγ ligand showed similar hemodynamic parameters when compared with vehicle-treated mature animals (Table 1). Histological examination of lung sections demonstrated that *in vivo* treatment with 15d-PGJ$_2$ (0.5 mg/kg i.p.) reduced the cell engorgement of alveolar spaces of young vehicle-treated rats subjected to hemorrhage (3 hrs) followed by resuscitation (3 hrs). However, lung architecture remained highly damaged in the mature group with large infiltration of inflammatory cells and hemorrhage (Fig. 7A–B; see Fig. 2 for histological comparison with vehicle-treated rats after hemorrhagic shock and sham control rats). Treatment with 15d-PGJ$_2$ (0.5 mg/kg) significantly reduced myeloperoxidase

activity in the lung of young rats, but it did not affect neutrophil infiltration in mature rats (Fig. 7C). In order to rule out whether the lack of effect of 15d-PGJ_2 on myeloperoxidase activity in mature rats might be due to the dose used, we treated a group of rats with a higher dose of the drug (1 mg/kg i.p.). However, even this higher dosage of 15d-PGJ_2 was unable to provide an effect on neutrophil infiltration in mature rats (Fig. 7C).

Effect of the PPARγ Ligand 15d-PGJ_2 on Lung NF-κB, PPARγ and HSF-1 DNA Binding

To elucidate the mechanisms accounting for the protective effects of 15d-PGJ_2 in young animals, DNA binding of PPARγ, NF-κB and HSF-1 was determined in lung nuclear extracts. Treatment with 15d-PGJ_2 caused an early increase of PPARγ DNA binding (i.e., at 15 and 30 min after resuscitation), which was associated with significant reduction of DNA binding activity of NF-κB when compared with vehicle treatment in young rats. Treatment with 15d-PGJ_2 also caused a significant increase in DNA binding of HSF-1 in young rats in comparison with vehicle-treated rats. In contrast, administration of 15d-PGJ_2 to the mature animals did not affect DNA binding of PPARγ, NF-κB or HSF-1 when compared to vehicle-treated mature rats (Fig. 8).

DISCUSSION

The co-morbidity of chronic inflammatory diseases, health habits and the different therapeutic management of trauma victims may concur with the clinical variability of lung injury in adults when compared to pediatric patients. The likelihood of developing MODS also depends on the magnitude of the initial insult (2). However, since no predictable correlation exists between the initial trauma event and the occurrence of MODS, it is possible that other intrinsic factors of the victim are involved and may be age-dependent. Our study demonstrates that the severity of the systemic inflammatory response and lung injury during hemorrhagic shock is age-dependent and is regulated at the nuclear level by changes in expression and function of PPARγ and by changes of its interaction with other signal transduction pathways. Specifically, we have demonstrated that PPARγ is downregulated in the lung as a function of age under normal physiological conditions. After severe hemorrhage, in older rats there is a further marked suppression of PPARγ expression and activation, which correlates with acute lung injury. This age-dependent response appears to be secondary to a diverse regulation of the signaling pathways of NF-κB and HSF-1. Treatment with 15d-PGJ_2, a PPARγ ligand, represses the inflammatory response in the lung of young animals but fails to achieve cytoprotective effects in adult animals.

To mimic the clinical situation of severe trauma in adult and pediatric patients we have chosen an experimental model of hemorrhagic shock in young and mature rats. Although it is difficult to establish the exact correlation of the human age versus the rodent age, longevity and growth are considered reliable operational criteria to select a model for age-related investigations (20). Since the median life length for a population of Wistar rats ranges from 26 to 29 months (21), it is plausible that young rats (3–5 months old) may correspond to a pediatric population of 8–14 years old, while mature rats (11–13 months old) may correspond to an adult human population of 35–50 years old. In this experimental setting, the amount of blood loss and, therefore, the degree of hypoperfusion may also contribute to the severity of the inflammatory response. To avoid this variability, we adopted a model of pressure-controlled hemorrhage (22), which allowed maintaining a low constant mean arterial blood pressure (50 mmHg for 3 hrs) to induce hypoperfusion. In our study, age-related changes in hemodynamic parameters were evident under basal conditions, and were consistent with changes observed by others in the rat (23–25). Mature animals were hypertensive, with slower HR and decreased CI and SVI when compared with young animals. Nevertheless, the sequential cardiovascular response to hemorrhage was similar in both age groups and was characterized by a marked decline (50–

60%) in CI and SVI, while TPRI and HR were maintained. In both age groups, blood replacement appeared to partially restore MABP via increase in CI rather than TPRI, thus suggesting that cardiac function was still preserved. Although it has been reported that age-related cardiovascular changes in aging animals do not alter mass perfusion rate in tissues under basal conditions (26), we cannot rule out that blood flow distribution in major organs might differ during hemorrhage and contribute to injury. Nevertheless, our results provide evidence that in the experimental population (i.e., 11–13 months old) age may be an independent risk factor of the overwhelming inflammatory response in hemorrhagic shock, further supporting the clinical findings observed in humans >55 years old (27).

Previously, we have reported that PPARγ expression is a function of the inflammatory response, as PPARγ is downregulated in the bronchial epithelium and in the endothelium of thoracic aortas in rats subjected to polymicrobial sepsis (11). PPARγ expression and DNA binding are also markedly reduced in lungs of mice subjected to endotoxic shock and are associated with massive lung injury and neutrophil infiltration (12,13). Other laboratories also support the hypothesis that PPARγ is downregulated during inflammation. PPARγ expression is reduced in adipose tissue (9) and in the heart (28) in mice subjected to endotoxin administration, and in the liver of rats subjected to sepsis by cecal ligation and puncture (29) or double-hit hemorrhage and sepsis (30). In this current study, we found that lung expression of PPARγ was also a function of age. After hemorrhage, lung PPARγ expression markedly declined in both young and mature rats; however this downregulation was more pronounced in mature animals and was associated with a more severe inflammatory response when compared to young animals. Interestingly, kinetics of PPARγ DNA binding did not exactly reflect the kinetics of protein expression as evaluated by Western blot analysis. These data suggest that other factors, other than total nuclear availability of the protein, may also regulate binding activity of PPARγ during hemorrhagic shock, such as availability of endogenous ligands and alteration of protein conformation by post-translational mechanisms. However, because of the age-dependent scarce availability of the receptor in mature rats, the treatment with the PPARγ ligand 15d-PGJ_2 did not afford any protective effect after severe hemorrhage even at very high dosages. On the contrary, in our study, 15d-PGJ_2 ameliorated lung injury in young rats. Treatment with 15d-PGJ_2 also ameliorated MABP, without altering other hemodynamic parameters, in the young group only. Similar beneficial effects of PPARγ ligands have been reported in hemorrhagic shock in experimental young animals (31–33).

It has been proposed that PPARγ plays a crucial role in the control of the inflammatory response by complex interactions with other signaling mechanisms (8). One potential anti-inflammatory mechanism of PPARγ involves the transrepression of the NF-κB pathway (8). The role of NF-κB as an important nuclear regulator in the development of acute lung injury has previously been described during hemorrhagic shock (4–6). Further studies have suggested the pathophysiological role of NF-κB, since *in vivo* NF-κB inhibition can afford protective effects in rodents subjected to severe hemorrhage (34–36). In our study, we have demonstrated that nuclear binding of NF-κB is a very early event during hemorrhage and resuscitation and precedes infiltration of neutrophils in the lung. Interestingly, the degree of DNA binding for NF-κB was diminished in young rats when compared to mature animals. *In vivo* treatment with the PPARγ ligand 15d-PGJ_2 further reduced this binding in young rats. However, in our study we did not completely define the inhibitory mechanism of 15d-PGJ_2 on NF-κB activation. Our previous experiments have shown that the anti-inflammatory properties of 15d-PGJ_2 are also secondary to inhibition of the upstream inhibitor κBα kinase (IKK) (11). Of interest, we have recently observed that PPARγ has a direct inhibitory effect on IKK, and ciglitazone, another PPARγ ligand, affords lung protection by maintaining a PPARγ/IKK complex during hemorrhagic shock in young rats (33). Furthermore, we cannot exclude that PPARγ may modulate other signaling pathways. In this regard, we have previously reported that PPARγ ligands reduce vascular nitrosative injury in young rats with sepsis (11), and reduce expression

of the inducible nitric oxide synthase in cultured macrophages (37). These beneficial effects are associated with inhibition of the IKK/NF-κB (11,37) and the c-Jun aminoterminal kinase/activator protein-1 pathways (11). Thus, our data suggest that the inflammatory response differs in young and mature animals depending also on the level of NF-κB activation, which may additionally alter the expression of inflammatory mediators. Our data also suggest that the age-dependent alteration of NF-κB activation may inversely correlate with PPARγ activation.

Several age-dependent impaired endothelial dysfunctions may contribute to the neutrophil sequestration into the lung. Aging is associated with a reduction in the regenerative capacity of the endothelium and endothelial senescence (38). In our study, we observed that ICAM-1 expression is increased in the lung of older animals. Of note, expression of this adhesion molecule had a multiphasic pattern and did not exactly reflect kinetics of MPO activity. Our findings are in agreement with previous reports demonstrating that senescent smooth vascular muscle and endothelial cells overexpress ICAM-1 in aged vessels (39,40). Our data also support previous studies demonstrating that lung ischemia and reperfusion had a biphasic effect on ICAM-1 protein expression, with an early initial decrease secondary to high superoxide generation and a late-phase increase, which did not parallel neutrophil accumulation (41).

To explore the role of other mediators in neutrophil recruitment, we also measured levels of chemokines and cytokines in the plasma. Although we did not confirm their tissue levels, it appears that the increases of systemic plasma cytokines and chemokines, including IL-6 and IL-1β, well reflect local increases of lung levels, as it has been recently reported in a rodent model of hemorrhagic shock and resuscitation under conventional ventilation (similar to the model used in our study) (42). In our study, we observed a discrepancy between high levels of chemokines and reduced leukocyte infiltration in the lung of young animals. This differential functional response to chemokines, nevertheless, is supported by several studies. For example, it appears that KC does not play a predominant role in the lung migration and activation of neutrophils during this inflammatory event. In agreement with this latter hypothesis, it has been reported that *in vivo* gene silencing of pulmonary KC does not inhibit hemorrhage-induced, neutrophil-mediated septic acute lung injury (43). On the contrary other studies have shown that increases in intravascular levels of IL-8, the human analogue of KC, impede neutrophil recruitment to inflammatory foci (44). Similarly to our data, the levels of MCP-1 in dermal wounds of aged burned mice were approximately half the levels of young animals, but there was no difference in macrophage accumulation into the wound between young and aged mice (45). MCP-1 expression and production in monocyte/macrophages from rats at normoxic conditions was reduced in aged subjects (46). This decline in chemokine production has been also reported in human aging, as natural killer lymphocytes of elderly subjects exhibit a gradual decline in the ability to produce IL-8 (47). Thus, taken together with these previous reports, our data suggest that in mature animals changes in ICAM-1 expression, most probably secondary to oxidative stress, and changes in chemokine production alter cellular recruitment in the lung.

The heat shock response is a highly conserved defense mechanism that provides cytoprotection from oxidative stress and ischemia-reperfusion injury. In eukaryotic cells, the production of HSPs is regulated at the transcriptional level by HSF-1 (7,17,48). Experimental studies have shown that hemorrhagic shock is associated with the expression of inducible HSPs, especially HSP72, in liver, brain, heart, and kidney. Furthermore, prior induction of HSP72 expression before the onset of shock is associated with an attenuation of organ injury caused by hemorrhage (49). In addition, *in vitro* studies have shown that the expression of HSP72 is decreased in senescent cells, indicating that the process of aging may be associated with reduced heat shock response (50). In line with these reports, in our study we have found that DNA binding activity of HSF-1, which controls the cytoprotective heat shock response, is more pronounced in lungs of young rats when compared to mature animals subjected to hemorrhage

and resuscitation. *In vivo* treatment with the PPARγ ligand 15d-PGJ_2 further enhances DNA binding of HSF-1 in young lungs.

Our *in vivo* findings are in agreement with previous reports demonstrating that cyclopentenone prostaglandins may induce expression of HSPs in the lung during endotoxic shock (12) and in the heart during ischemia and reperfusion injury (15). However, it has been proposed that the effect of 15d-PGJ_2 on HSF-1 may be independent of PPARγ activation and may be attributed to the chemical characteristics of the cyclopentenone ring (51). Nevertheless, other PPARγ ligands, such as thiazolidinediones, share this ability to induce the heat shock response and to exert anti-inflammatory effects in spinal cord injury (52) and pancreatitis (53). Thus, induction of the heat shock response may represent an important anti-inflammatory mechanism of PPARγ ligands. Interestingly, in our study treatment with 15d-PGJ_2 did not affect HSF-1 binding in mature lungs following hemorrhage. Although further studies are needed to determine the exact mechanisms of action 15d-PGJ_2 on the heat shock response, our data suggest that an age-dependent downregulation of the heat shock response occurs during the development of lung injury following hemorrhage and parallels with the decline of PPARγ activation.

CONCLUSION

Our study is the first observation that age-related differences exist in the pattern of PPARγ expression and activation, as well as NF-κB and HSF-1 activation. Of clinical interest, pharmacological PPARγ activation may afford protective effects in the lung of young animals. These protective effects are associated with inhibition of NF-κB and enhancement of HSF-1 binding. In contrast, treatment with a PPARγ ligand fails to afford protection in older animals. Thus, these data suggest that activation of the endogenous PPARγ pathway may represent a therapeutic means to counteract the lung injury in a clinical setting of trauma and exsanguination. However, as a person ages, cytoprotective interventions may need to be tailored to the specific conditions that predominate in the aged population.

Acknowledgments

Financial support: Supported by the National Institutes of Health to Dr. Basilia Zingarelli (grant R01 GM-067202; R01 AG-27990). No additional potential conflicts of interest have been disclosed.

References

1. Calkins CM, Bensard DD, Moore EE, et al. The injured child is resistant to multiple organ failure: a different inflammatory response? J Trauma 2002;53:1058–1063. [PubMed: 12478028]
2. Sauaia A, Moore FA, Moore EE, et al. Multiple organ failure can be predicted as early as 12 hours after injury. J Trauma 1998;45:291–301. [PubMed: 9715186]
3. Scannell G, Waxman K, Tominaga GT. Respiratory distress in traumatized and burned children. J Pediatr Surg 1995;30:612–614. [PubMed: 7595846]
4. Moine P, Shenkar R, Aneko D, et al. Systemic blood loss affects NF-κB regulatory mechanisms in the lungs. Am J Physiol Lung Cell Mol Physiol 1997;273:L185–L192.
5. Shenkar R, Abraham E. Mechanisms of lung neutrophil activation after hemorrhage or endotoxemia: roles of reactive oxygen intermediates, NF-κB, and cyclic AMP response element binding protein. J Immunol 1999;163:954–962. [PubMed: 10395692]
6. Kim JY, Park JS, Strassheim D, et al. HMGB1 contributes to the development of acute lung injury after hemorrhage. Am J Physiol Lung Cell Mol Physiol 2005;288:L958–L965. [PubMed: 15640285]
7. Wheeler DS, Wong HR. Heat shock response and acute lung injury. Free Radic Biol Med 2007;42:1–14. [PubMed: 17157189]
8. Zingarelli B, Cook JA. Peroxisome proliferator-activated receptor-γ is a new therapeutic target in sepsis and inflammation. Shock 2005;23:393–399. [PubMed: 15834303]

9. Hill MR, Young MD, McCurdy CM, et al. Decreased expression of murine PPARγ in adipose tissue during endotoxemia. Endocrinology 1997;138:3073–3076. [PubMed: 9202256]
10. Tanaka T, Itoh H, Doi K, et al. Down regulation of peroxisome proliferator-activated receptor-γ expression by inflammatory cytokines and its reversal by thiazolidinediones. Diabetologia 1999;42:702–710. [PubMed: 10382590]
11. Zingarelli B, Sheehan M, Hake PW, et al. Peroxisome proliferator activator receptor-γ agonists, 15-deoxy-$\Delta^{12,14}$-PGJ_2 and ciglitazone, reduces systemic inflammation in polymicrobial sepsis by modulation of signal transduction pathways. J Immunol 2003;171:6827–6837. [PubMed: 14662889]
12. Kaplan JM, Cook JA, Hake PW, et al. 15-Deoxy-$\Delta^{12,14}$-prostaglandin J_2 (15d-PGJ_2), a peroxisome proliferator activated receptor γ ligand, reduces tissue leukosequestration and mortality in endotoxic shock. Shock 2005;24:59–65. [PubMed: 15988322]
13. Vish MG, Hake PW, O'Connor M, et al. Proinsulin C-peptide exerts beneficial effects in endotoxic shock in mice. Crit Care Med 2007;35:1348–1355. [PubMed: 17414724]
14. Liu D, Zeng BX, Zhang SH, et al. Rosiglitazone, a peroxisome proliferator-activated receptor-γ agonist, reduces acute lung injury in endotoxemic rats. Crit Care Med 2005;33:2309–2316. [PubMed: 16215386]
15. Zingarelli B, Hake PW, Mangeshkar P, et al. Diverse cardioprotective signaling mechanisms of peroxisome proliferator-activated receptor-γ ligands, 15-deoxy-$\Delta^{12,14}$-prostaglandin J_2 and ciglitazone, in reperfusion injury: role of nuclear factor-κB, heat shock factor 1, and Akt. Shock 2007;28:554–563. [PubMed: 17589386]
16. Zingarelli B, Ischiropoulos H, Salzman AL, et al. Amelioration by mercaptoethylguanidine of the vascular and energetic failure in haemorrhagic shock in the anesthetised rat. Eur J Pharmacol 1997;338:55–65. [PubMed: 9408003]
17. Goldenberg CJ, Luo Y, Fenna M, et al. Purified human factor activates heat shock promoter in a HeLa cell-free transcription system. J Biol Chem 1988;263:19734–19739. [PubMed: 3198647]
18. Martinez-Mier G, Toledo-Pereyra LH, Ward PA. Adhesion molecules and hemorrhagic shock. J Trauma 2001;51:408–415. [PubMed: 11493811]
19. Zingarelli B, Sheehan M, Wong HR. Nuclear factor-κB as a therapeutic target in critical care medicine. Crit Care Med 2003;31:S105–S111. [PubMed: 12544984]
20. Masoro EJ. Use of rodents as models for the study of "normal aging": conceptual and practical issues. Neurobiol Aging 1991;12:639–643. [PubMed: 1791898]
21. Masoro EJ. Mortality and growth characteristics of rat strains commonly used in aging research. Exp Aging Res 1980;6:219–233. [PubMed: 7398709]
22. Majde JA. Animal models for hemorrhage and resuscitation research. J Trauma 2003;54:S100–S105. [PubMed: 12768110]
23. Labat C, Cunha RS, Challande P, et al. Respective contribution of age, mean arterial pressure, and body weight on central arterial distensibility in SHR. Am J Physiol Heart Circ Physiol 2006;290:H1534–H1539. [PubMed: 16243913]
24. Pacher P, Mabley JG, Liaudet L, et al. Left ventricular pressure-volume relationship in a rat model of advanced aging-associated heart failure. Am J Physiol Heart Circ Physiol 2004;287:H2132–H2137. [PubMed: 15231502]
25. Weisfeldt M. Aging, changes in the cardiovascular system, and responses to stress. Am J Hypertens 1998;11:41S–45S. [PubMed: 9546036]
26. Delp MD, Evans MV, Duan C. Effects of aging on cardiac output, regional blood flow, and body composition in Fischer-344 rats. J Appl Physiol 1998;85:1813–1822. [PubMed: 9804586]
27. Sauaia A, Moore FA, Moore EE, et al. Early predictors of postinjury multiple organ failure. Arch Surg 1994;129:39–45. [PubMed: 8279939]
28. Feingold K, Kim MS, Shigenaga J, et al. Altered expression of nuclear hormone receptors and coactivators in mouse heart during the acute-phase response. Am J Physiol Endocrinol Metab 2004;286:E201–E207. [PubMed: 14701665]
29. Siddiqui AM, Cui X, Wu R, et al. The anti-inflammatory effect of curcumin in an experimental model of sepsis is mediated by up-regulation of peroxisome proliferator-activated receptor-γ. Crit Care Med 2006;34:1874–1882. [PubMed: 16715036]

30. Higuchi S, Wu R, Zhou M, et al. Downregulation of hepatic cytochrome P-450 isoforms and PPAR-γ: their role in hepatic injury and proinflammatory responses in a double-hit model of hemorrhage and sepsis. J Surg Res 2007;137:46–52. [PubMed: 17101152]
31. Collin M, Abdelrahman M, Thiemermann C. Endogenous ligands of PPARγ reduce the liver injury in haemorrhagic shock. Eur J Pharmacol 2004;486:233–235. [PubMed: 14975712]
32. Abdelrahman M, Collin M, Thiemermann C. The peroxisome proliferator-activated receptor-γ ligand 15-deoxy$\Delta^{12,14}$ prostaglandin J_2 reduces the organ injury in hemorrhagic shock. Shock 2004;22:555–561. [PubMed: 15545828]
33. Chima R, Hake P, Mangeshkar P, et al. Ciglitazone ameliorates lung inflammation by modulating the IKK/NF-κB pathway following hemorrhagic shock. Crit Care Med 2008;36:2849–2857. [PubMed: 18828195]
34. Yang R, Gallo DJ, Baust JJ, et al. Ethyl pyruvate modulates inflammatory gene expression in mice subjected to hemorrhagic shock. Am J Physiol Gastrointest Liver Physiol 2002;283:G212–G221. [PubMed: 12065309]
35. McDonald MC, Mota-Filipe H, Paul A, et al. Calpain inhibitor I reduces the activation of nuclear factor-κB and organ injury/dysfunction in hemorrhagic shock. FASEB J 2001;15:171–186. [PubMed: 11149905]
36. Zingarelli, B.; Hake, PW.; Burroughs, T., et al. Parthenolide, an inhibitor of NF-κB, reduces the inflammatory response in hemorrhagic shock in the rat. Proceedings of: The Sixth World Congress on Trauma, Shock, Inflammation and Sepsis - Pathophysiology, Immune Consequences and Therapy; March 2–6, 2004; Munich, Germany. Medimond S.r.l., Bologna, Italy. 2004. p. 193-198.
37. Piraino G, Cook JA, O'Connor M, et al. Synergistic effect of peroxisome proliferator activated receptor-γ and liver X receptor-α in the regulation of inflammation in macrophages. Shock 2006;26:146–153. [PubMed: 16878022]
38. Yildiz O. Vascular smooth muscle and endothelial functions in aging. Ann NY Acad Sci 2007;1100:353–360. [PubMed: 17460198]
39. Minamino T, Miyauchi H, Yoshida T, et al. Endothelial cell senescence in human atherosclerosis: role of telomere in endothelial dysfunction. Circulation 2002;105:1541–1544. [PubMed: 11927518]
40. Kletsas D, Pratsinis H, Mariatos G, et al. The proinflammatory phenotype of senescent cells: the p53-mediated ICAM-1 expression. Ann NY Acad Sci 2004;1019:330–332. [PubMed: 15247038]
41. Lu YT, Chen PG, Liu SF. Time course of lung ischemia-reperfusion-induced ICAM-1 expression and its role in ischemia-reperfusion lung injury. J Appl Physiol 2002;93:620–628. [PubMed: 12133872]
42. Bouadma L, Dreyfuss D, Ricard JD, et al. Mechanical ventilation and hemorrhagic shock-resuscitation interact to increase inflammatory cytokine release in rats. Crit Care Med 2007;35:2601–2606. [PubMed: 17828032]
43. Lomas-Neira JL, Chung CS, Wesche DE, et al. In vivo gene silencing (with siRNA) of pulmonary expression of MIP-2 versus KC results in divergent effects on hemorrhage-induced, neutrophil-mediated septic acute lung injury. J Leukoc Biol 2005;77:846–853. [PubMed: 15695553]
44. Simonet WS, Hughes TM, Nguyen HQ, et al. Long-term impaired neutrophil migration in mice overexpressing human interleukin-8. J Clin Invest 1994;94:1310–1319. [PubMed: 7521886]
45. Shallo H, Plackett TP, Heinrich SA, et al. Monocyte chemoattractant protein-1 (MCP-1) and macrophage infiltration into the skin after burn injury in aged mice. Burns 2003;29:641–647. [PubMed: 14556721]
46. Reale M, Di Giulio C, Cacchio M, et al. Oxygen supply modulates MCP-1 release in monocytes from young and aged rats: decrease of MCP-1 transcription and translation is age-related. Mol Cell Biochem 2003;248:1–6. [PubMed: 12870648]
47. Mariani E, Pulsatelli L, Meneghetti A, et al. Different IL-8 production by T and NK lymphocytes in elderly subjects. Mech Ageing Dev 2001;122:1383–1395. [PubMed: 11470128]
48. Stephanou A, Latchman DS. Transcriptional regulation of the heat shock protein genes by STAT family transcription factors. Gene Expr 1999;7:311–319. [PubMed: 10440232]
49. De Maio A. Heat shock proteins: facts, thoughts, and dreams. Shock 1999;11:1–12. [PubMed: 9921710]

50. Liu AY, Lin Z, Choi HS, et al. Attenuated induction of heat shock gene expression in aging diploid fibroblasts. J Biol Chem 1989;264:12037–12045. [PubMed: 2745427]

51. Rossi A, Elia G. Santoro MG: 2-Cyclopenten-1-one, a new inducer of heat shock protein 70 with antiviral activity. J Biol Chem 1996;271:32192–32196. [PubMed: 8943275]

52. Park SW, Yi JH, Miranpuri G, et al. Thiazolidinedione class of peroxisome proliferator-activated receptor γ agonists prevents neuronal damage, motor dysfunction, myelin loss, neuropathic pain, and inflammation after spinal cord injury in adult rats. J Pharmacol Exp Ther 2007;320:1002–1012. [PubMed: 17167171]

53. Konturek PC, Dembinski A, Warzecha Z, et al. Pioglitazone, a specific ligand of peroxisome proliferator-activated receptor-γ, protects pancreas against acute cerulein-induced pancreatitis. World J Gastroenterol 2005;11:6322–6329. [PubMed: 16419161]

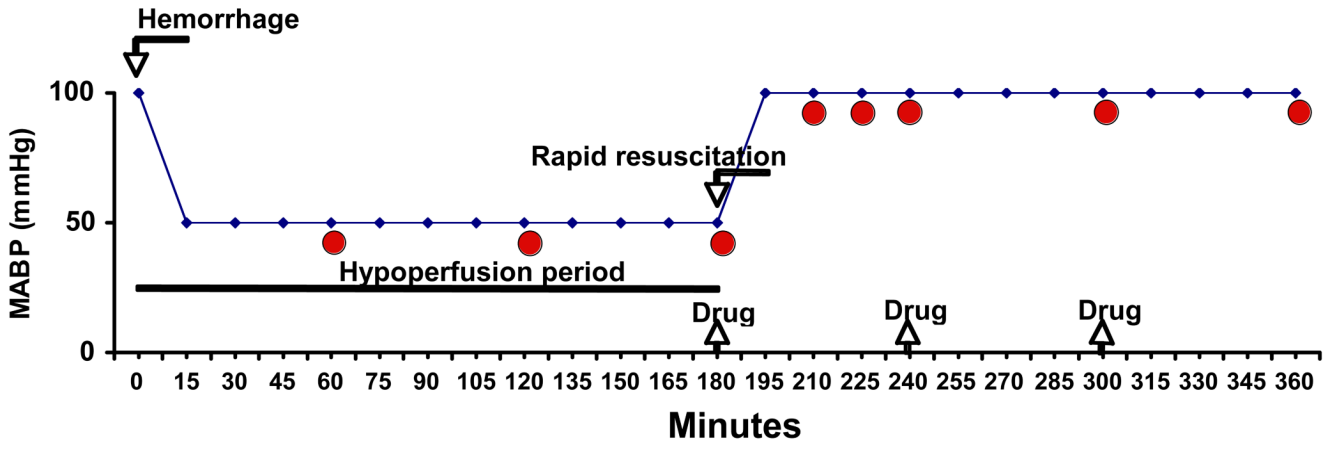

Figure 1.

Schematic representation of hemorrhagic shock model. Curved arrows indicate timing of blood removal (Hemorrhage) and blood replacement (Rapid resuscitation); straight arrows indicate timing of treatment with vehicle or 15d-PGJ_2 (Drug); circles indicate timing of sacrifice and tissue collection.

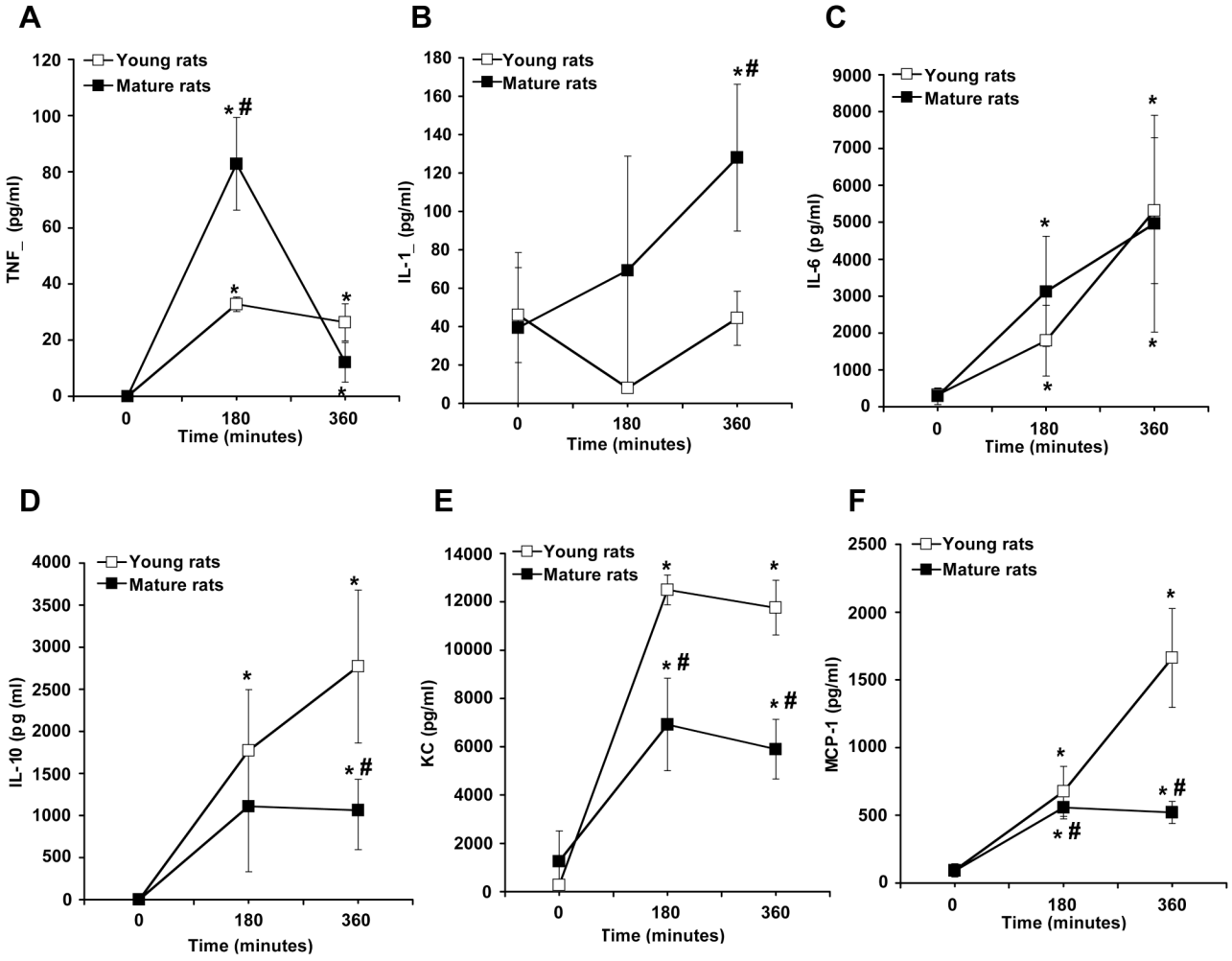

Figure 2.

Plasma levels of TNFα (*A*), IL-1β (*B*), IL-6 (*C*), IL-10 (*D*), KC (*F*) and MCP-1 (*E*) in young and mature rats. Each data point represents the mean ± SEM of 4–7 rats for each group at basal level (time 0), at the end of hemorrhage (180 min) and at the end of resuscitation (360 min). *Represents $p <. 05$ *versus* basal levels of same age group rats. #Represents $p <.05$ *versus* young rats at the same time point.

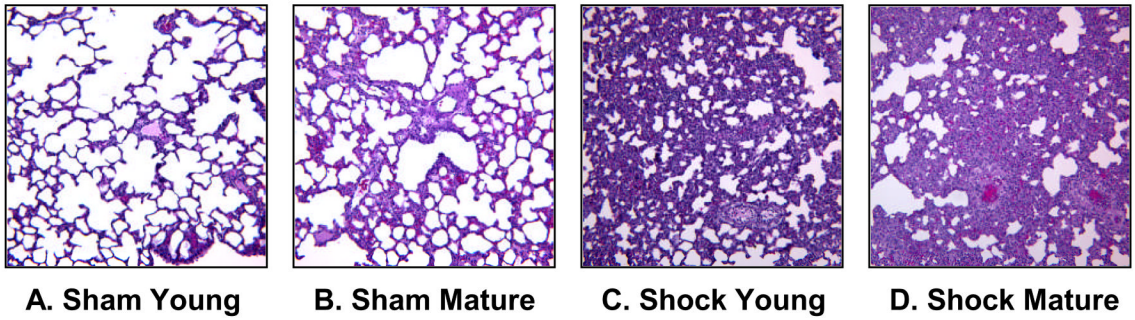

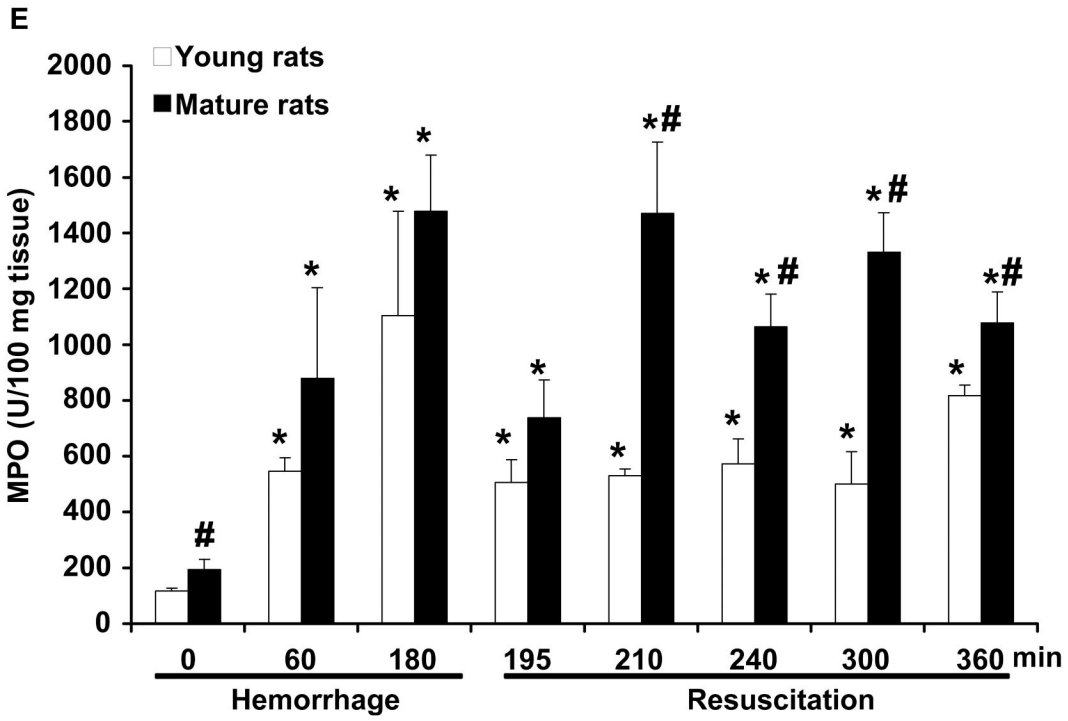

Figure 3.

Representative histology of lung sections stained with hematoxylin and eosin. Lung architecture in sham young (*A*) and sham mature rat (*B*). Architectural alterations in a young rat (*C*) and a mature rat (*D*) following hemorrhage (3 hrs) and resuscitation (3 hrs). Magnification x 100. A similar pattern was seen in n=5–10 lung sections in each experimental group. (*E*) Lung myeloperoxidase (MPO) activity in young and mature rats at basal conditions (time 0 in sham animals) and after hemorrhage and resuscitation. Each data point represents the mean ± SEM of 9–16 rats for each group. *Represents $p <$. 05 *versus* basal levels of same age group rats. #Represents $p <$.05 *versus* young rats at the same time point.

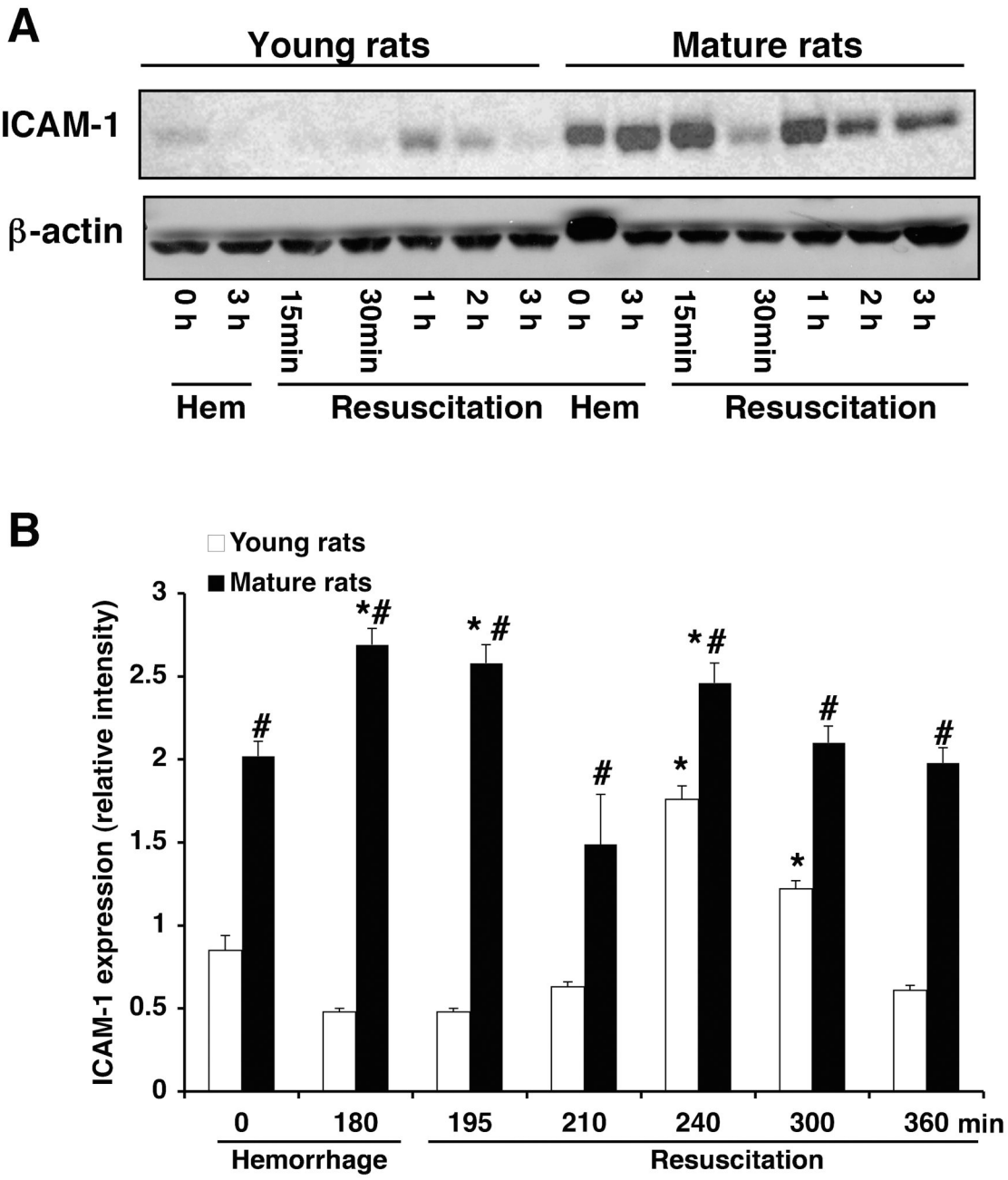

Figure 4.

(*A*) Western blot analysis of ICAM-1 expression (top panel) in lungs of young and mature rats after hemorrhage and resuscitation. Fifty μg proteins were loaded for each lane. Equal loading was confirmed by β-actin immunoblotting (bottom panel). Results are representative of 3 separate time-course experiments. (*B*) Lung ICAM-1 expression as determined by densitometry from the radiographs. Fold increase was normalized versus respective β-actin value. Each data point represents the mean ± SEM of 3 separate time-course experiments. *Represents $p <$. 05 *versus* basal levels of same age group rats. #Represents $p <$.05 *versus* young rats at the same time point.

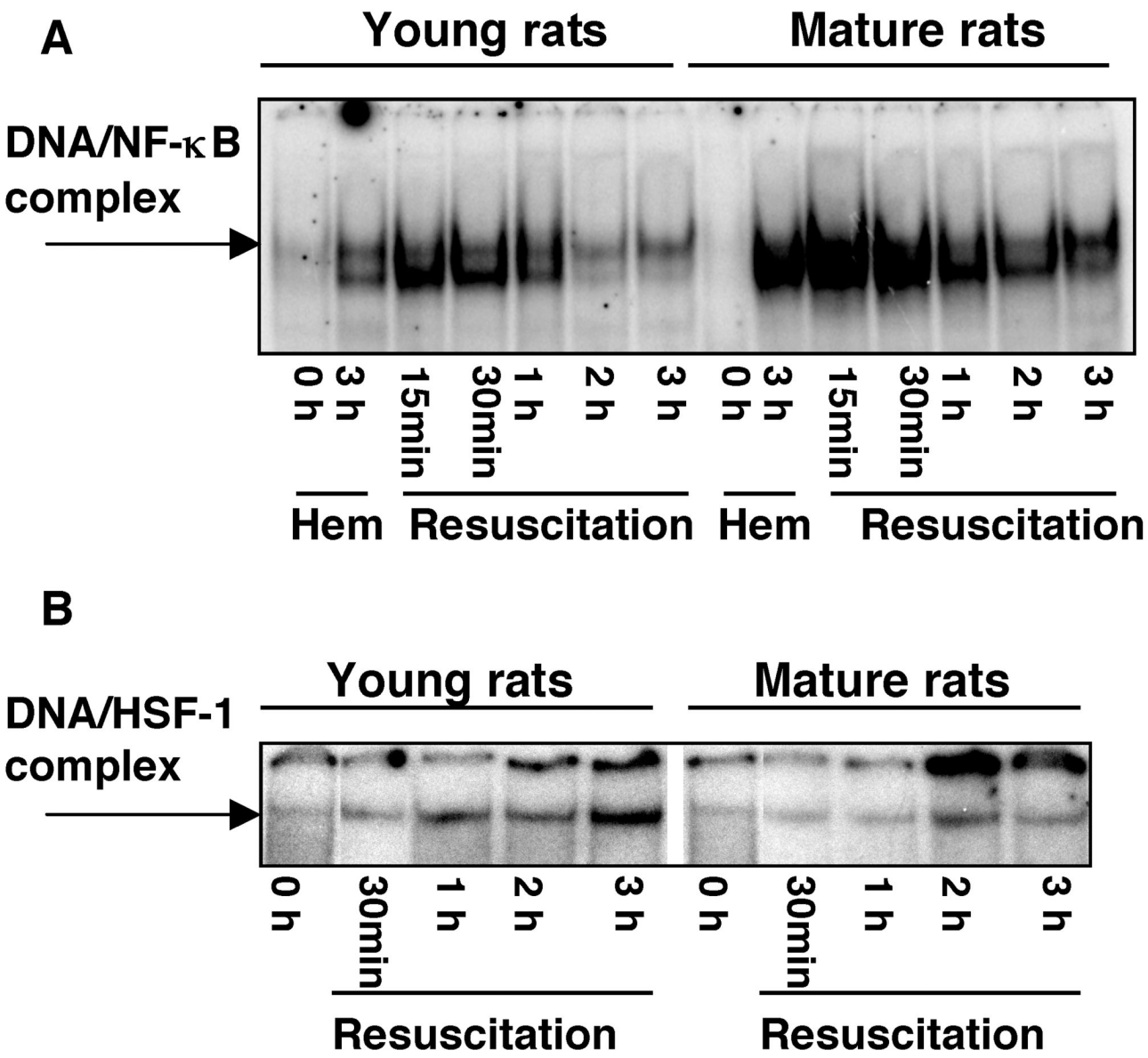

Figure 5.
Time course of DNA binding of NF-κB (*A*) and HSF-1 (*B*) in the lung of young and mature rats subjected to hemorrhage and resuscitation as evaluated by EMSA. Autoradiograph is representative of 3 separate time-course experiments.

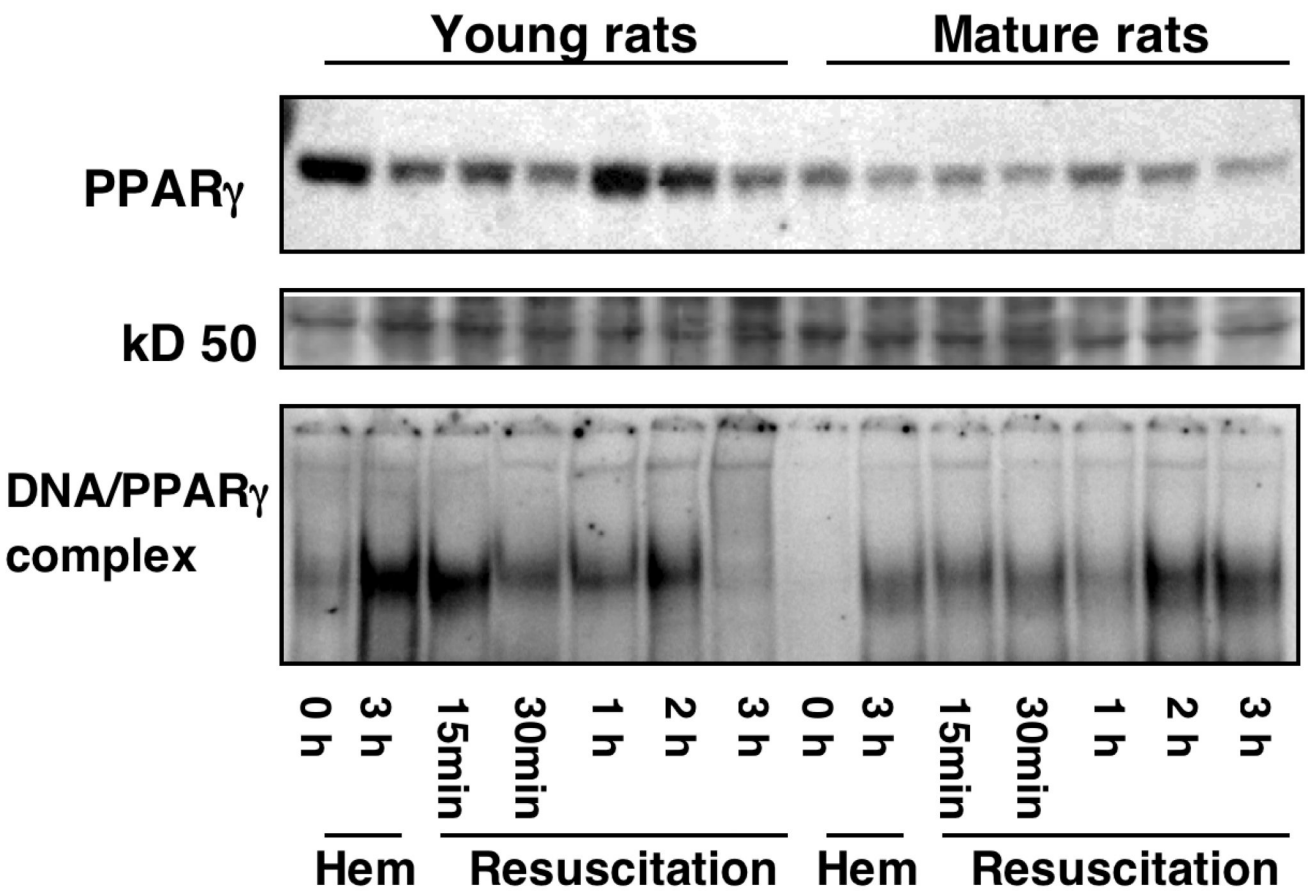

Figure 6.
Western blot of nuclear PPARγ expression (*top panel*) in the lung of young and mature rats subjected to hemorrhage and resuscitation. Equal loading was confirmed by Ponceau staining after transfer of proteins on nitrocellulose membrane (a 50 kD protein is shown for representation, *middle panel*). *Bottom panel*, DNA binding of PPARγ in the lung of young and mature rats subjected to hemorrhage and resuscitation as evaluated by EMSA. Radiographs are representative of 3 separate time-course experiments.

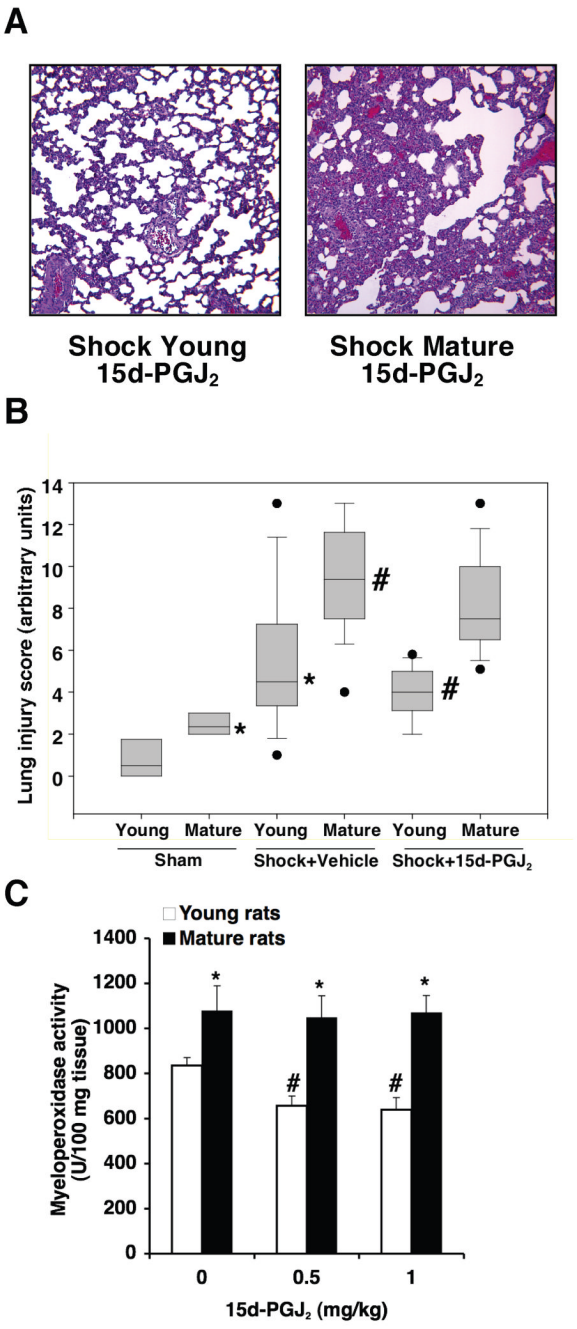

Figure 7.

(*A*) Representative lung histology of a young and a mature rat subjected to hemorrhage (3 h) and resuscitation (3 h) and treated with 15d-PGJ_2 (0.5 mg/kg i.p.). For comparison with vehicle-treated rats and sham groups see Figure 2. Magnification x 100. A similar pattern was seen in n=10 lung sections in each experimental group. (*B*) Histopathological scores of lung sections (of n=5–10 rats for each group). Lung injury was scored from 0 (no damage) to 16 (maximum damage). Box plots represent 25th percentile, median and 75th percentile; error bars define 10th and 90th percentile; black dots define outliers. *Represents $p < .05$ *versus* young sham rats. #Represents $p < .05$ *versus* young vehicle-treated rats subjected to hemorrhagic shock. Treated rats received 15d-PGJ_2 (0.5 mg/kg i.p.). (*C*) Effect of treatment with 15d-PGJ_2 (0.5–

1 mg/kg i.p.) on lung myeloperoxidase activity in young and mature rats subjected to hemorrhage (3 h) and resuscitation (3 h). Each data point represents the mean ± SEM of 5–16 rats for each group. *Represents $p < .05$ *versus* young rats. #Represents $p < .05$ *versus* vehicle-treated rats (i.e., 0 mg/kg).

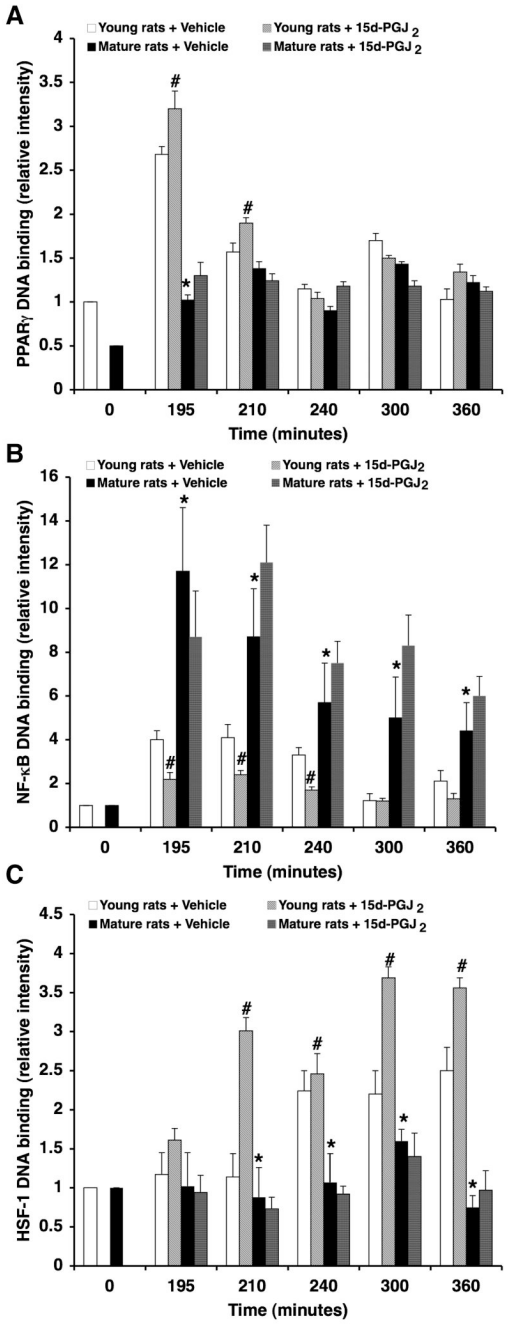

Figure 8.

Effect of treatment with 15d-PGJ_2 (0.5 mg/kg i.p.) on lung DNA binding of PPARγ (*A*), NF-κB (*B*) and HSF-1 as determined by densitometry from EMSA autoradiographs. Fold increase was calculated versus respective sham value (time 0) set to 1.0. Each data point represents the mean ± SEM of 3 separate time-course experiments. *Represents $p < .05$ *versus* young rats. #Represents $p < .05$ *versus* vehicle-treated rats.

Table 1

Hemodynamic parameters in young and mature rats at basal conditions (time 0, before hemorrhage) and at the end of the hemorrhage (180 min) and after resuscitation at (240, 300 and 360 min)

GROUPS	Time (*min*)	Treatment	MABP (*mmHg*)	HR (*beats/min*)	CI (*ml/min/100 g*)	TPRISVI (*mmHg/ml/min/100 g*)(*ml/100 g*)
Young rats	0	Vehicle	126.5±3.8	419.4±8.7	27.5±3.7	5.1±0.665.5±8.7
		15d-PGJ_2	132.9±6.0	417.8±9.0	23.4±3.0	6.8±1.155.6±6.7
during hemorrhage	180	Vehicle	50.9±4.0^{a}	404.6±15.0	11.2±1.3^{a}	5.4±1.028.3±3.9^{a}
		15d-PGJ_2	54.2±6.0	399.7±9.1	14.2±2.3	4.7±0.835.9±5.9
Young rats	240	Vehicle	90.9±4.5^{a}	461.9±18.5	18.3±2.4^{a}	7.0±2.139.9±5.7^{a}
		15d-PGJ_2	103.8±6.0^{c}	442.2±9.6	17.5±2.9	7.4±1.239.7±7.0
during resuscitation	300	Vehicle	85.8±4.9^{a}	422.3±17.4	16.5±3.4^{a}	8.4±2.539.1±8.0^{a}
		15d-PGJ_2	95.5±6.4^{c}	443.8±11.3	17.0±2.9	7.0±1.338.4±6.6
	360	Vehicle	78.4±5.5^{a}	394.3±20.0	15.2±2.7^{a}	5.4±0.742.0±6.1^{a}
		15d-PGJ_2	85.8±6.4^{c}	418.9±13.2	14.9±2.2	6.5±0.836.0±5.6
Mature rats	0	Vehicle	138.6±3.5^{b}	360.6±11.4^{b}	12.6±0.8^{b}	11.2±0.6^{b}35.4±2.4^{b}
		15d-PGJ_2	138.2±12.0	385.0±16.6	10.6±1.6	15.3±4.128.1±4.7
during hemorrhage	180	Vehicle	50.9±3.7^{a}	380.2±11.4^{b}	5.6±0.7^{ab}	11.5±1.5^{b}14.8±1.8^{ab}
		15d-PGJ_2	52.9±5.3	391.8±20.1	5.6±1.4	12.6±4.313.9±3.9
Mature rats	240	Vehicle	106.9±5.8^{ab}	397.0±15.7^{b}	12.0±1.9^{b}	11.8±1.4^{b}29.7±4.3^{b}
		15d-PGJ_2	116.4±10.3	440.6±26.9	13.7±3.1	11.2±4.030.1±5.6
during resuscitation	300	Vehicle	97.8±4.4^{ab}	408.4±10.6^{b}	12.1±1.9	10.9±1.6^{b}28.8±4.2^{b}
		15d-PGJ_2	83.8±12.0	397.8±24.7	10.0±1.4	10.3±0.721.9±6.1
	360	Vehicle	101.4±5.2^{ab}	405.1±12.9	11.8±2.0	10.0±1.2^{b}29.1±3.9^{b}
		15d-PGJ_2	99.6±13.6	444.0±28.5	9.9±1.3	10.4±2.122.2±6.1

Values are means ± S.E.M. for 5–35 rats per group. MABP, mean arterial blood pressure; HR, heart rate; CI, cardiac index; TPRI, total peripheral resistance index; SVI, stroke volume index. Hemodynamic parameters were recorded before hemorrhage (basal at time 0), at the end of hemorrhage (180 min) and after resuscitation (at 240, 300 and 360 min).

^{a} $p <$ .05 *versus* basal levels (time 0) of same age group rats

^{b} $p <$ .05 *versus* young rats

[c] $p < .05$ *versus* vehicle treatment.